

Dissipative Particle Dynamics with Energy Conservation: Heat Conduction

Marisol Ripoll⁽¹⁾ *, Pep Español⁽¹⁾, and Matthieu H. Ernst⁽²⁾

⁽¹⁾*Dep. Física Fundamental, UNED, Apt. 60141, 28080 Madrid, Spain*

⁽²⁾*Institute for Theoretical Physics, Utrecht University, Princetonplein 5, P.O. Box 80.006, 3508 TA Utrecht, The Netherlands*

We study by means of numerical simulations the model of dissipative particle dynamics with energy conservation for the simple case of thermal conduction. It is shown that the model displays correct equilibrium fluctuations and reproduces Fourier law. The connection between “mesoscopic coarse-graining” and “resolution” is clarified.

I. INTRODUCTION

Mesoscopic approaches to the study of complex fluids are receiving a great deal of attention in view of their potential to address problems with disparate time-scales. The method of dissipative particle dynamics introduced originally as an hybrid between lattice gas and molecular dynamics simulations [1], has proven to be a flexible and powerful tool in the study of complex fluids as colloidal suspensions [2–4], porous flow [1], polymer suspensions [5], and multicomponent flows [6].

DPD models a fluid as a collection of point particles that are interpreted as representing the center of mass of a mesoscopic cluster of the atoms or molecules that constitute the fluid. By formulating physically motivated interactions (that is, dissipative forces that conserve momentum [1,7]) between these “lumps” of fluid, it is assured that the macroscopic behavior of the system is hydrodynamic [8,9]. Most importantly, a random interaction is introduced in order to account for thermal fluctuations that occur at the mesoscopic level and are responsible for Brownian effects appearing in complex fluids.

One of the drawbacks of classic DPD is that the total energy of the system is not conserved because the forces are velocity dependent. This has been recently remedied simultaneously and independently in Refs. [10,11], where an internal energy variable and a temperature is introduced for each particle. The mechanical energy that is dissipated due to the velocity dependent forces is transformed into internal energy of the particles. This viscous heating process is accompanied by a thermal conduction process where exchange of internal energy between neighboring particles occurs when differences of temperatures exist. The new DPD algorithm with energy conservation opens up the possibility of studying not only rheological aspects of complex fluids but also thermal issues. It is therefore important to validate the technique in simple situations for which the dynamical aspects are well-known, either analytically or by means of other numerical simulations techniques.

As a first step towards the understanding of the behavior of DPD with energy conservation we focus in this paper on the simplest problem of conduction in a quiescent fluid (or a solid). This is a particular case of the model introduced in Refs. [10,11]. The particles are at rest and located randomly and represent portions of material that can interchange energy. This simple model can be regarded as a way of solving a fluctuating heat conduction equation. In section 2 we review the model that was introduced in Refs. [10,11], for the case that only heat conduction takes place. In section 3 we further specify the model functions. In section 4 we present simulation results that show the validity of the simulation method by comparing the numerical results with the theoretical results. Finally, we end up with a section of conclusions.

II. THE MODEL

We have introduced in Ref. [10] a mesoscopic model for describing a fluctuating viscous and thermally conducting fluid. Here we apply this model to a quiescent fluid (or solid) within a box. The system is represented by a set of N particles of fixed positions \mathbf{r}_i which are distributed at random within the box. These particles are understood as thermodynamic subsystems of the whole system, that is, small portions of material that have a sufficiently large number of degrees of freedom. To each particle we associate an internal energy variable ϵ_i an entropy function $s(\epsilon_i)$, and a temperature $T_i^{-1} = \partial s_i / \partial \epsilon_i$. Each particle represents a mesoscopic portion of the material and its internal energy content is subject to thermal fluctuations, which in a continuum theory would be described by a random heat

*e-mail: mripoll@fisfun.uned.es, pep@fisfun.uned.es, ernst@phys.uu.nl

flux. [12] Differences in temperatures between neighboring particles will cause a transfer of internal energy. Therefore, the following stochastic differential equation for the internal energy of each particle is postulated

$$d\epsilon_i = \sum_j \omega(r_{ij}) \kappa_{ij} \left(\frac{1}{T_i} - \frac{1}{T_j} \right) dt + \sum_j (2k_B \omega(r_{ij}) \kappa_{ij})^{1/2} dW_{ij}^\epsilon \quad (1)$$

The first term in the r.h.s. is deterministic and specifies that a temperature difference causes exchange of energy. The second term is stochastic and takes into account thermally induced fluctuations in each particle caused by a random interchange of energy between particles. The notation is as follows. k_B is Boltzmann's constant, $r_{ij} = |\mathbf{r}_i - \mathbf{r}_j|$ is the distance between particles i, j and the dimensionless weight function $\omega(r)$ determines the range of influence between particles. The parameter κ_{ij} governs the overall amplitude of the deterministic and random parts. It depends in general on the state variables of particles i, j and is symmetric under particle interchange. The random "heat flux" from particle i to j is expressed in terms of the increments of the Wiener process dW_{ij}^ϵ . The increments of the Wiener process are antisymmetric under particle interchange $dW_{ij}^\epsilon = -dW_{ji}^\epsilon$ in such a way that the total internal energy of the system governed by Eqn. (1) is exactly conserved $\frac{d}{dt} \sum_i \epsilon_i = 0$. Because κ_{ij} might depend in general on ϵ_i, ϵ_j we need to provide a stochastic interpretation of Eqn. (1), as the noise is multiplicative. We choose Itô interpretation. It has been shown that, if $\partial_{ij} \kappa_{ij} = 0^1$, then Eqn. (1) is mathematically equivalent to a Fokker-Planck equation which has as equilibrium solution

$$\rho_{eq}(\epsilon) \propto \exp \left\{ k_B^{-1} \sum_i s(\epsilon_i) \right\} \mathcal{P}(\sum_k \epsilon_k) \quad (2)$$

where $\mathcal{P}(\sum_k \epsilon_k)$ is a function of the total internal energy which is determined by the initial distribution of total energy. Particular examples are given by the canonical [11] and microcanonical ensembles

$$\begin{aligned} \rho_{mic}(\epsilon_1, \dots, \epsilon_N) &= \frac{1}{\Omega(E_0, N)} \exp \left\{ k_B^{-1} \sum_i s(\epsilon_i) \right\} \delta(\sum_i \epsilon_i - E_0) \\ \rho_{can}(\epsilon_1, \dots, \epsilon_N) &= \frac{1}{Z(\beta, N)} \exp \left\{ k_B^{-1} \sum_i s(\epsilon_i) - \beta \epsilon_i \right\} \end{aligned} \quad (3)$$

Here, the factors $\Omega(E_0, N)$ and $Z(\beta, N)$ are obtained by normalization.

III. PERFECT SOLID AND FOURIER LAW

In this section we further specify the model by providing the undetermined functions $T(\epsilon)$, $\kappa(\epsilon + \epsilon')$ and $\omega(r)$ appearing in Eqn. (1).

The simplest possible form for the equation of state $T(\epsilon)$ is that of a perfect solid, which is a very good approximation for metals. The perfect solid has the following equation of state

$$T(\epsilon) = \frac{\epsilon}{C_v} \quad (4)$$

where the heat capacity of the mesoscopic particles C_v is a constant independent of the energy. It is an extensive property that depends on the "size" of the particles. For mesoscopic particles, the dimensionless heat capacity $\alpha \equiv C_v/k_B \gg 1$. The entropy $s(\epsilon)$ is obtained by integrating the temperature and, apart from irrelevant constant additive terms, it is given by $s(\epsilon) = C_v \ln \epsilon$.

Now, let us assume the following functional form for κ_{ij} ,

$$\kappa_{ij} = \frac{C_v \tilde{\kappa}}{\lambda^2} T^2 \left(\frac{\epsilon_i + \epsilon_j}{2} \right) = \frac{C_v \tilde{\kappa}}{4\lambda^2} (T_i + T_j)^2 \quad (5)$$

¹This implies that if κ_{ij} depends only on ϵ_i, ϵ_j then, necessarily, it will be a function of $\epsilon_i + \epsilon_j$. This can be proved by considering a Taylor expansion of a function of two variables and using the fact that, at each point, both partial derivatives coincide.

where λ is the average distance between particles (this is $\lambda = n^{-1/3}$ and n is the average density number) and $\tilde{\kappa}$ has dimensions of a diffusion coefficient. In the last equality, Eqn. (4) has been used.

Substitution of Eqn. (5) into the dynamical equation for the energy leads to the following equation for the temperature of a particle

$$dT_i = \frac{\tilde{\kappa}}{\lambda^2} \sum_j \omega(r_{ij}) \frac{(T_i + T_j)^2}{4T_i T_j} (T_j - T_i) dt + \left(\frac{2k_B \tilde{\kappa}}{C_v \lambda^2} \right)^{1/2} \sum_j \omega^{1/2}(r_{ij}) \frac{T_i + T_j}{2} dW_{ij}^\epsilon \quad (6)$$

The factor $\frac{(T_i + T_j)^2}{4T_i T_j}$ should be very close to 1 if the temperature differences between particles within an action sphere are small. We see, then, that for the perfect solid by a proper selection of κ_{ij} the form of the postulated SDE for the energy leads to a discrete version of the Fourier law of heat conduction. Note that the factor λ^2 in the first term of the left hand side of Eqn. (6) can be understood as the “lattice spacing” squared that would arise in a finite difference discretization of the Laplacian in the heat conduction equation. In a sense, Eqn. (6) can be understood as a finite difference discretization of the macroscopic heat equation on a *random* lattice which, in addition, has the correct form for the thermal fluctuations.

We will assume that the weight function $\omega(r)$ has the form of the Lucy weight function [13], which is a smooth bell-shaped function with continuous derivatives. It is given by

$$\omega(r) = \frac{105}{16\pi s^3} \left(1 + 3\frac{r}{r_c} \right) \left(1 - \frac{r}{r_c} \right)^3 \quad (7)$$

where r_c is range of interaction between particle and $s = r_c/\lambda$ is the *overlapping coefficient* which gives, essentially, the number of neighbors of a given particle. We have normalized the weight function as [1]

$$\int d^d \mathbf{r} \omega(r) = \frac{1}{n} \quad (8)$$

IV. SIMULATION RESULTS

In this section we present some results obtained from numerical simulation of Eqn. (6). The physical system is assumed to be in a three dimensional cubic box of edge length L . Initially the box is seeded with N mesoscopic particles located at random. The density is then $n = N/L^3$ and the typical interparticle distance is $\lambda = n^{-1/3}$. Periodic boundary conditions are assumed in the y, z directions and in the x direction we assume either periodic boundary conditions when considering equilibrium situations or we impose the temperature at $x = -L/2$ and $x = L/2$. This is achieved by considering two extra layers of particles in each boundary in the x direction filled with particles that are at a constant temperature. These layers act, therefore, as *thermal baths*. They have a width as large as r_c in order that any particle within the system interacts with the same number of particles.

The basic model parameters are the following ones: $\tilde{\kappa}$, N , L , r_c , C_v , T_0 . Here, T_0 is a reference temperature, that of equilibrium or, in the case of nonequilibrium situations, that of the colder thermal bath. We work in reduced units such that L is the unit of length, $L^2/\tilde{\kappa}$ is unit of time, T_0 is the unit of temperature, and k_B is taken as the unit of entropy or heat capacity.

We introduce the dimensionless heat capacity of mesoscopic particles $\alpha = C_v/k_B$ and the dimensionless heat capacity of the total simulated sample, which is $C_L = N\alpha$ because heat capacity is an extensive property. On the other hand, $C_L = L^3 c_v/k_B$, where c_v is the heat capacity per unit volume, which is a material constant. For example, $c_v = 3.44 \times 10^6 J/Km^3$ for copper at room temperature. Therefore, by fixing C_L we are fixing the actual volume of the sample. For copper, a value $C_L = 10^8$ implies a submicron sample size of $L = C_L^{1/3} \times 1.610^{-10} m \sim 0.1 \mu$. In most of the simulations we use $C_L = 10^8$ and this fixes the value of α depending on the number of particles in the system. Note that by fixing C_L , large N implies small α , in accordance with the idea that the heat capacity of the mesoscopic particles is proportional to its typical size. We note that the overall intensity of the noise in (6) is proportional to $(k_B/C_v)^{1/2} = \alpha^{-1/2}$ and, therefore, inversely proportional to the square root of the volume of the particles. [14] The higher the number density of mesoscopic particles used to discretize a given sample, the smaller is the size of such particles and, therefore, the larger is the thermal noise.

Eqns. (6) are solved with a conventional Euler method. For values of $\alpha < 10$, the stochastic term produces from time to time a temperature which is negative for some particle. This has disastrous consequences because the factor accompanying $(T_i - T_j)$ in the deterministic term of (6) is negative and produces a flow of energy from the cold

particles to the hot particles. When this happens the system becomes unstable. However, this never occurs for sufficiently large values of α as the ones we typically use and no instabilities are observed.

In order to check that the code performs properly, we first run a simulation with fully periodic boundary conditions. Initially, all the particles are assumed to have the same temperature $T = 1$. After some equilibration period the system reaches equilibrium. The energy is exactly conserved (no round-off errors) because we use a Verlet list [15], in such a way that what is gained by a particle is exactly what is lost by the rest of particles.

In Fig. 1 we show the probability density distribution of the energy of a particle as obtained from simulation of Eqn. (1) for two different values of $\alpha = C_v/k_B$, the dimensionless heat capacity of the mesoscopic particles, for a system of $N = 1000$. The larger α the larger the average value of the energy and variance. However, the relative fluctuations are smaller, proportional to $N^{-1/2}$. Also shown in Fig. 1 are the canonical $f_{\text{can}}(\epsilon)$ and microcanonical $f_{\text{mic}}(\epsilon)$ theoretical results for the given values of α . The analytical expressions can be obtained from (3) and are given by

$$\begin{aligned} f_{\text{can}}(\epsilon) &= \frac{\beta}{\Gamma(\alpha + 1)} (\beta\epsilon)^\alpha \exp\{-\beta\epsilon\} \\ f_{\text{mic}}(\epsilon) &= \frac{1}{M} \frac{1}{E_0} \left(\frac{\epsilon}{E_0}\right)^\alpha \left(1 - \frac{\epsilon}{E_0}\right)^{(N-1)(\alpha+1)-1} \end{aligned} \quad (9)$$

where $\Gamma(x)$ is the gamma function. The parameter β can be explicitly computed for a perfect solid by requiring that the average energy of a particle is E_0/N , where E_0 is the total energy of the isolated system. The result is $\beta = N(\alpha + 1)/E_0$. In the thermodynamic limit the canonical and microcanonical distributions are identical. In practice, they are indistinguishable for values $N\alpha > 50$. The perfect coincidence of the theoretical and simulation results in Fig. 1 gives confidence on the implementation of the numerical code used.

Next, we compute the thermal diffusivity by a macroscopic measurement. Two heat baths are constructed with temperatures T_{cold} and T_{hot} in such a way that a gradient $(T_{\text{hot}} - T_{\text{cold}})/L$ is applied. A steady state is reached for sufficiently long times. Fig. 2 shows the average of the temperature once the steady state has been reached for different number of particles for the case that $T_{\text{cold}} = 1$, $T_{\text{hot}} = 2$ and the overlapping coefficient is $s = 1.5$. For $N = 100$ the spatial noise is considerable. Fluctuations in this graph are not due to statistical noise but to the spatial inhomogeneities that appear for small number of particles and they would smear out by averaging over different realizations of the initial spatial configuration of the particles. For larger number of particles a smooth linear profile is achieved, in accordance with our expectation that the discrete model reproduces Fourier law. The temperature field $T(x)$ is obtained by binning the x axis and averaging the temperatures of the particles within each bin of volume $\Delta x L^2$.

We have performed a series of simulations with different temperature gradients and have computed the macroscopic heat flux in the steady state. Two different ways of computing the macroscopic heat flux have been used. In the first case, the macroscopic heat flux is obtained by computing at each time step the energy gained by the cold bath (which is equal to the energy lost by the hot bath) and dividing it by the time step, this is $\Delta E/\Delta t$. The second way follows from the microscopic definition of the heat flux as obtained from projection operator methods or from kinetic theory [16]

$$\mathbf{Q} \equiv \sum_{ij} \omega(r_{ij}) \kappa_{ij} \left[\frac{1}{T_i} - \frac{1}{T_j} \right] \frac{\mathbf{r}_{ij}}{2} \quad (10)$$

All transport fluxes are caused by collisional transfer. As the particles do not move, there are no kinetic fluxes. This second form produces better results because it involves a very large number of pairs of particles and it is therefore adopted here.

In Fig. 3 we plot the macroscopic heat flux in terms of the applied temperature gradient. A linear dependence is obtained, which allows to extract the thermal diffusivity from the slope.

When this experiment is performed for different number densities and different overlapping we can compare with the results from kinetic theory as developed in Ref. [16]. Fig. 4 shows the value of the macroscopic thermal diffusivity as a function of the overlapping s . Also shown is the kinetic theory prediction for the thermal diffusivity [16], reading,

$$D = \frac{s^2}{24} \tilde{\kappa} \quad (11)$$

We observe that the theoretical prediction improves for large overlapping.

The kinetic theory result (11) has been obtained through the choices Eqns. (4) and (5) and shows no dependence on the density. This is a consequence of introducing the factor λ^{-2} in Eqn. (5). We verify in Fig. 5 that simulations performed at different number density, with the remaining parameters s, C_L held fixed, show that the thermal diffusivity D is indeed independent of n , as predicted in Eqn. (11).

V. CONCLUSIONS

In this paper we have applied the model introduced in Ref. [10] to the case of heat conduction in a random solid. We have chosen the equation of state $s(\epsilon_i)$ for a perfect solid model and a particular model for κ_{ij} , Eqn. (5). It has been shown that the model has the correct equilibrium properties and that it reproduces Fourier's law in non-equilibrium situations. We have also corroborated, by means of simulations, the kinetic theory predictions for this model which are presented elsewhere. Kinetic theory predicts a thermal diffusivity which depends only on the overlapping and not on the density. By introducing the factor λ^{-2} in the definition of κ_{ij} we have shown that it is possible to interpret n not as the density but as the *resolution* at which the physical problem is being studied. A similar discussion about resolution was presented for the case of DPD with no energy conservation in Ref. [17].

ACKNOWLEDGMENTS

M.R. acknowledges the support of a F.P.I. grant from Ministerio de Educación. P.E. has received partial support from DGICYT Project No PB94-0382 and by E.C. Contract ERB-CHRXCT-940546.

REFERENCES

-
- [1] P.J. Hoogerbrugge and J.M.V.A. Koelman, Europhys. Lett. **19**, 155 (1992).
 - [2] J.M.V.A. Koelman and P.J. Hoogerbrugge, Europhys. Lett. **21**, 369 (1993).
 - [3] E.S. Boek, P.V. Coveney, H.N.W. Lekkerkerker, and P. van der Schoot, Phys. Rev. E **55**, 3124 (1997).
 - [4] E.S. Boek, P.V. Coveney, and H.N.W. Lekkerkerker, J. Phys.: Condens. Matter **8**, 9509 (1997).
 - [5] A.G. Schlijper, P.J. Hoogerbrugge, and C.W. Manke, J. Rheol. **39**, 567 (1995).
 - [6] P.V. Coveney and K. Novik, Phys. Rev. E **54**, 5134 (1996).
 - [7] P. Español and P. Warren, Europhys. Lett. **30**, 191 (1995).
 - [8] P. Español, Phys. Rev. E, **52**, 1734 (1995).
 - [9] C. Marsh, G. Backx, and M.H. Ernst, Europhys. Lett. **38**, 411 (1997). C. Marsh, G. Backx, and M.H. Ernst, Phys. Rev. E **56**, 1976 (1997).
 - [10] P. Español, Europhys. Lett. **40**, 631 (1997).
 - [11] J. Bonet Avalós and M. Mackie, Europhys. Lett. **40**, 141 (1997).
 - [12] L.D. Landau and E.M. Lifshitz, *Fluid Mechanics* (Pergamon Press, 1959).
 - [13] L.B. Lucy, Astron. J. **82**, 1013 (1977).
 - [14] P. Español, Physica A **248**, 77 (1997).
 - [15] M.P. Allen and D.J. Tildesley, *Computer Simulation of Liquids* (Clarendon Press, Oxford, 1987).
 - [16] M. Ripoll, M.H. Español, and M.H. Ernst, preprint.
 - [17] P. Español, Phys. Rev. E **57**, 2930 (1998).

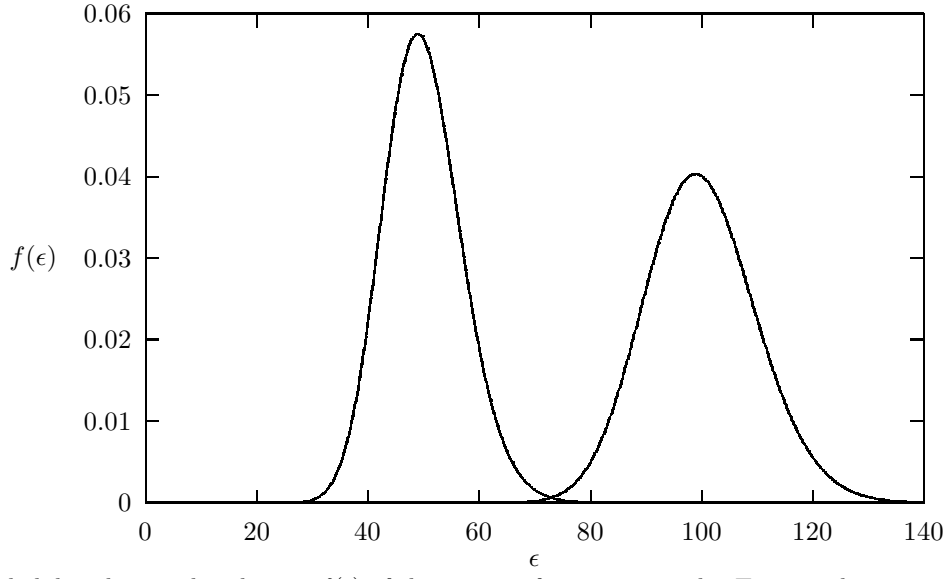


FIG. 1. The probability density distribution $f(\epsilon)$ of the energy of a given particle. Two simulations with $\alpha = 50$ (left) and $\alpha = 100$ (right) are presented. Other parameters are $N = 1000$, $s = 1.5$, $T_{eq} = 1$. Also shown, although not visible because they are perfectly superimposed, are the theoretical predictions for the microcanonical and canonical distributions for the given values of α .

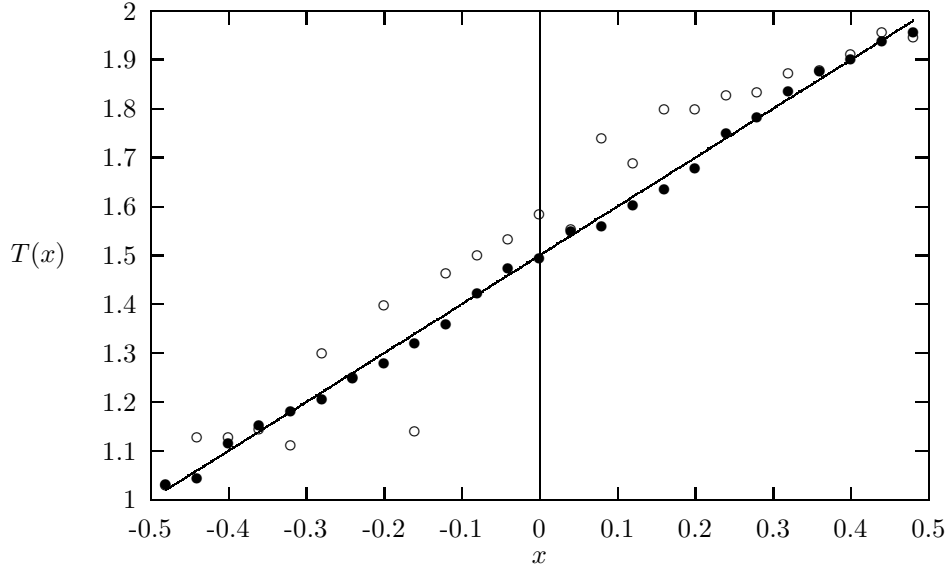


FIG. 2. Average temperature of the particles in each of the 25 bins in which the x axis of the box has been divided. Solid line is the theoretical Fourier profile. Open circles correspond to $N = 100$ and solid circles correspond to $N = 1000$ particles within the box. Other parameters are $s = 1.5$, $C_L = 10^8$.

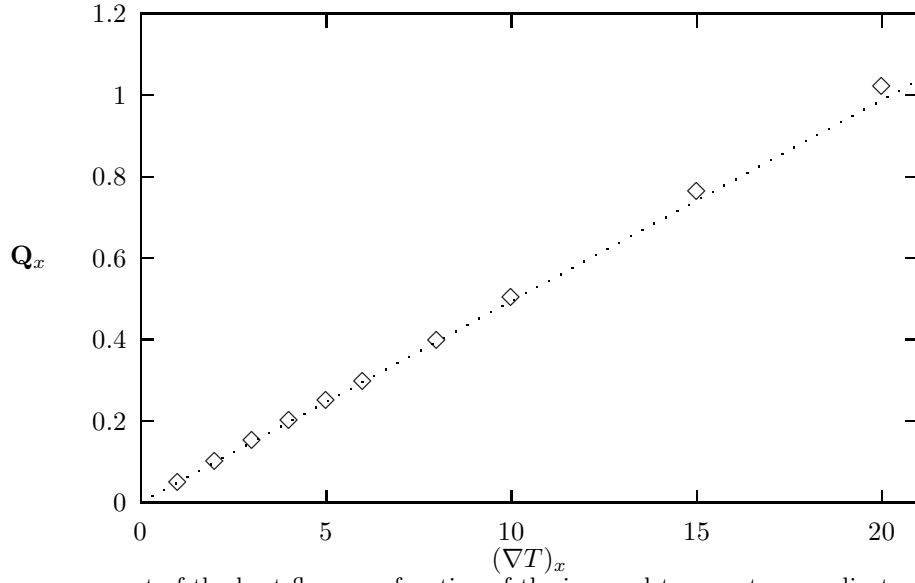


FIG. 3. Average x component of the heat flux as a function of the imposed temperature gradient. A linear dependence is obtained with small deviations at large gradients. The slope of the straight line gives the thermal diffusivity.

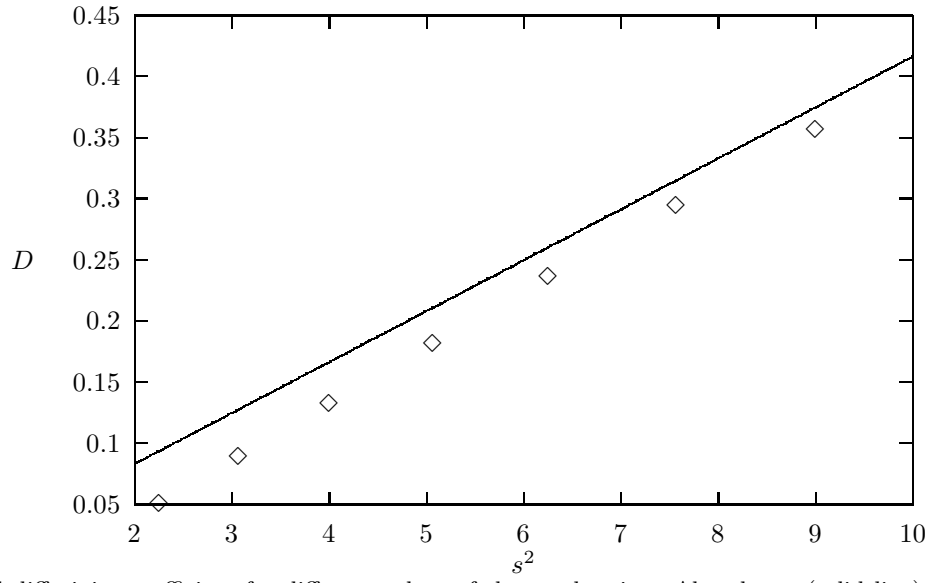


FIG. 4. Thermal diffusivity coefficient for different values of the overlapping. Also shown (solid line) is the kinetic theory prediction.

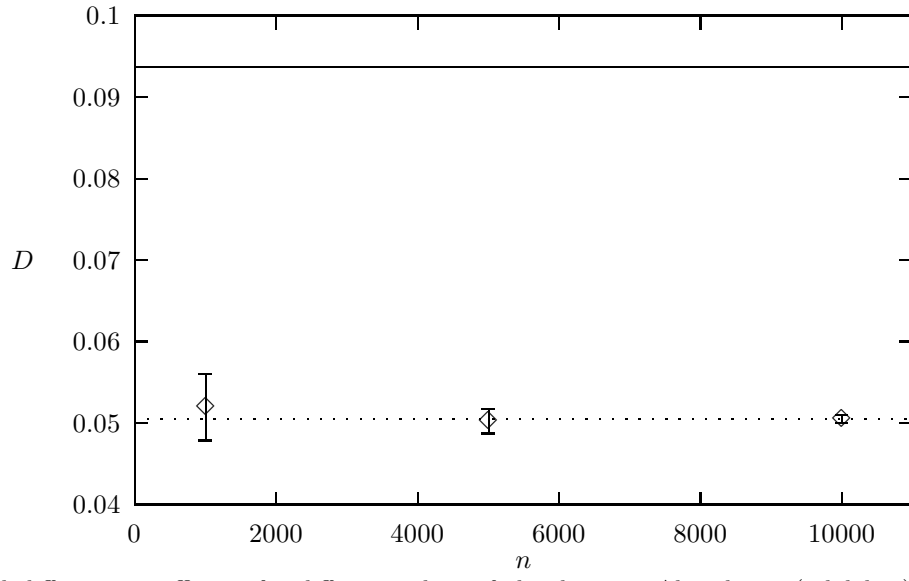


FIG. 5. Thermal diffusivity coefficient for different values of the density. Also shown (solid line) is the kinetic theory prediction for this value of the overlapping $s = 1.5$.